Shape Optimization of Cylindrical Shell for Interior Noise

Jay H. Robinson
NASA Langley Research Center
Hampton, VA 23681

Abstract

In this paper an analytic method is used to solve for the cross spectral density of the interior acoustic response of a cylinder with nonuniform thickness subjected to turbulent boundary layer excitation. The cylinder is of honeycomb core construction with the thickness of the core material expressed as a cosine series in the circumferential direction. The coefficients of this series are used as the design variable in the optimization study. The objective function is the space and frequency averaged acoustic response. Results confirm the presence of multiple local minima as previously reported and demonstrate the potential for modest noise reduction.

Introduction

Aircraft interior noise levels have been an ongoing concern to airline operators and aircraft manufacturers for many years. The concerns have primarily been those of speech interference, crew fatigue, and passenger comfort, the latter arising primarily in private/business aircraft and first class accommodations. Though there are currently no regulations on interior noise levels, airline operators have required guarantees from manufacturers on these levels. Some primary sources of interior noise that are currently being studied due to their strong interaction with aircraft structures are propeller, jet, boundary layer, and turbine noise, the latter being a primarily structure borne noise associated with rotor imbalances. Both propeller and turbine noise are primarily tonal in nature and have been the object of several recent structural acoustic optimization investigations.

Cunefare et. al. [1,2] have been working to develop the tools and methodology for performing structural-acoustic optimization with acoustic objectives and constraints using commercial finite and boundary element software. Most of their structures were typical ring frame and stringer stiffened shells and fuselages subjected to either propeller or engine excitation. They demonstrated the ability to obtain modest amounts of noise reductions in many of the structures they studied with little or no weight penalty. Another observation from their work was that the acoustic objective function had many local minima and thus all of their results were reported as ranges. The level of noise reduction obtained in all their investigations varied widely depending on the initial design state. One of their first reported results was for a thin aluminum monocoque shell and of particular interest to this investigation. In this study the shell was divided circumferentially into eighteen strips. The thicknesses of the shell within each of these areas became the design variables in the optimization study. For this idealized structure subjected to narrow band propeller noise interior noise reductions of 17 to 24 dB were obtained. Though this type of structural tailoring is impractical on thin isotropic material, the results were very good.

The use of honeycomb core materials in commercial aircraft offer some significant advantages over aluminum, however, several disadvantages are also evident. An all-composite honeycomb core structure tends to have inherently lighter damping than its aluminum counterpart. The result of this is a potential for higher noise levels in the aircraft interiors. Several investigations whose objective was to improve the structural acoustic performance of honeycomb core structures have since been reported. Tang et. al. [3,4], in a classical parametric study, showed that 'very' thick honeycomb structures had a more favorable high frequency transmission loss characteristic than either metallic, composite, or 'thin' honeycomb structures. This appeared to be a phenomenon related to the ratio of the membrane and bending wave speeds. The prospect of using the ability to tailor this form of construction to reduce the low frequency interior noise levels of aircraft cabins has been investigated by Fernholz and Robinson [5,6]. They used the lamination angles of the inner and outer face sheets of the honeycomb side walls of an aircraft fuselage as design variables. Results demonstrated that a modest two to three dB of noise reduction was obtainable for interior noise generated by structural excitation.

The present investigation will explore both the potential for interior noise reduction and the nature of the design space in thick honeycomb shells subjected to turbulent boundary layer (TBL) excitation where the honeycomb core thickness is the design variable. Specifically, an analytic solution for the interior noise of a thick honeycomb core shell will be obtained for the case when the shell core thickness is expanded in a cosine series as

$$H_{core}(\theta) = h_c \; + \; h_c \; F(\theta) \; = h_c \; + \; h_c \sum_{i=1}^{nmax} \; d_i \;\; Cos(i \; \theta) \tag{1}$$

where h_c is the nominal core thickness and d_i are the non-dimensional design variables. The objective function used in this study is similar to that used by Cunefare et. al. [1,2]. It is the space and frequency averaged spectral density function of the acoustic pressure. In the remainder of this paper the solutions for the shell and acoustic responses will be discussed followed by the formal statement of the constrained optimization problem. Results from two optimization experiments will then be presented and discussed with respect to the nature of the design space and the potential for noise reduction.

Solution to Shell Response

The basic geometry of the shell initially indicated that a simple Donnell-Mustari or possibly Love or first order shear theory would be sufficient. In these shell theories terms of the order shell thickness over shell radius are assumed small with respect to unity and the shell equations are greatly simplified. Though this ratio for the baseline shell used in this study was nearly fifty to one, a convergence study using natural frequency as the criterion indicated a general thick shell theory with at least first order shear deformation theory was required. The reason for this is the nature of the shell construction. The shell is constructed of a honeycomb core with face sheet. The core requires the inclusion of shear deformation theory and due to the overall construction it is permissible for the bending stiffness to be of the order of the membrane stiffness. This precluded the simplifications made in many shell theories.

The necessary shell response required to predict the interior noise when the shell is subjected to turbulent boundary layer noise is the cross spectral density of the shell displacements. If the shell displacements are assumed as a series of admissible functions, this cross spectral density function is reduced to the cross spectral density of the unknown coefficients of these functions. The cross spectral density matrix is determined from the equation

$$S_{aa}(\omega) \quad = H^{-1}(\omega)\; S_{pp}(\omega) \quad H^{-t}(\omega) \tag{2}$$

were S_{aa} is the standard notation for the matrix of cross spectral density functions of the vector of unknown a, $H^{-1}(\omega)$ and $H^{-t}(\omega)$ are the inverse and inverse transpose of the frequency response functions for a, and $S_{pp}(\omega)$ is given by

$$S_{pp}(\omega) = \int_0^L \int_0^{2\pi} \int_0^L \int_0^{2\pi} \Psi(\theta_1, x_1)\; e^{-\alpha \frac{\omega}{U_c}|x_1 - x_2|}\; e^{-\beta \frac{\omega}{U_c} R|\theta_1 - \theta_2|}\; e^{i \frac{\omega}{U_c}(x_1 - x_2)}\; \Phi(\omega)\Psi(\theta_2, x_1)\; R^2 d\theta_2\; dx_1 d\theta_1\; dx_2 \tag{3}$$

where the cylinder coordinates are x and θ, and L and $2\pi R$ are the length and circumference of the cylinder. Equation 3 is recognized as the expansion of Corcos' cross spectral density model [7] of the turbulent boundary layer pressure in terms of the admissible shell displacement functions, Ψ. The coefficients of the exponential decay terms, α and β, are .11 and .77 respectively. These are the same values as used by Tang [4]. The convection velocity of the TBL, U_c, is taken as 65% of the free stream velocity. This is taken as Mach .7. The responses in this investigation are normalized with respect to the autospectrum of the TBL loading, $\Phi(\omega)$, which is assumed to be constant over the frequency ranges used in this investigation.

The frequency response functions for the vector of unknowns, a, can be derived from the second variation of the functional $\int_{vol} (T \quad - U \;)\; dv$ where T is kinetic energy and U is the strain energy of the shell. The strain-displacement relationships used in this investigation are for a thick shear deformable shell [8], the discussion of which is precluded for brevity. The kinetic energy and the strain energy are formed in the usual manner by substituting the displacement functions into the inertia and strain expressions. The U, V, and W displacements in terms of the admissible shape functions and their coefficients are

$$U(x,r,\theta,t) = \sum_{m=0}^{\infty} Cos\left(\frac{m\;\pi\;x}{\mathrm{L}}\right) \left[\sum_{n=0}^{\infty} [u^c_{nm} + z\;\psi^c_{nm}]\, Cos\,(m\theta) + \sum_{n=1}^{\infty} [u^s_{nm} + z\;\psi^s_{nm}]\, Sin\,(m\theta)\right] e^{i\omega t} \tag{4a}$$

$$V(x,r,\theta,t) = \sum_{m=1}^{\infty} Sin\left(\frac{m\;\pi\;x}{\mathrm{L}}\right) \left[\sum_{n=1}^{\infty} [v^c_{nm} + z\;\phi^c_{nm}]\, Sin\,(m\theta) + \sum_{n=0}^{\infty} [v^s_{nm} + z\;\phi^s_{nm}]\, Cos\,(m\theta)\right] e^{i\omega t} \tag{4b}$$

$$W(x,r,\theta,t) = \sum_{m=1}^{\infty} Sin\left(\frac{m\;\pi\;x}{\mathrm{L}}\right) \left[\sum_{n=0}^{\infty} w^c_{nm} Cos\,(m\theta) + \sum_{n=1}^{\infty} w^s_{nm} Sin\,(m\theta)\right] e^{i\omega t} \tag{4c}$$

where u^c_{nm}, u^s_{nm}, v^c_{nm}, v^s_{nm}, w^c_{nm}, w^s_{nm}, ψ^c_{nm}, ψ^s_{nm}, ϕ^c_{nm}, and, ϕ^s_{nm} are the unknowns which comprise the vector of unknowns, a. The shapes satisfy the classic shear diaphragm boundary conditions and for uniform cylinders permit an exact solution. The superscripts c and s denote the exact cosine theta and sine theta solutions and the subscripts n and m denote the wave number in the circumferential and longitudinal directions respectively.

The integration of the functional is carried out in a layer by layer manner since the cylinder is of laminated construction. The variable thickness of the cylinder wall, figure 1, is introduced in the limits of the integration in z which is the shell coordinate normal to the mid-surface of the shell defined by the midsurface of the shell, $r = R$. This integration takes the form

$$\int_{vol} (T-V)\ dv = \int_0^L \int_0^{2\pi} \left[\int_{-\frac{h_c}{2}-h_f+F(\theta)}^{-\frac{h_c}{2}+F(\theta)} (T-V) \left(1+\frac{z}{R}\right) dz + \int_{-\frac{h_c}{2}+F(\theta)}^{\frac{h_c}{2}} (T-V) \left(1+\frac{z}{R}\right) dz + \int_{\frac{h_c}{2}}^{\frac{h_c}{2}+h_f} (T-V) \left(1+\frac{z}{R}\right) dz \right] R\ d\theta\ dx \tag{5}$$

where the function $F(\theta)$ is given in equation 1, the incremental volume, dv, is $R\ \left(1+\frac{z}{R}\right) dz\ d\theta\ dx$, and h_f is the thickness of the face sheets. The integrations in z yield terms of first, second, third, fourth, and log order in $F(\theta)$. To facilitate the analytic evaluation of the integrals in theta the logarithmic terms are approximated to fourth order in $F(\theta)$. As previously stated, now that the integrals have been evaluated, the matrix of frequency response functions is determined from the second variation of the functional. A viscous damping term is added to the frequency response function matrix and the cross spectral density matrix of the response is solved using equation 2.

Acoustic Solution

The acoustic response inside the cylinder is governed by the damped wave equation. The wave equation can be written

$$\frac{\partial^2}{\partial t^2} P(r,\theta,x,t) + C_o^2\ (1+i\ \eta_a)\ \nabla^2\ P(r,\theta,x,t) = 0 \tag{6}$$

were Co is the speed of sound inside the cylinder and η_a is, by structural analogy, representative of the damping in the fluid. The solution for equation (6) is well known. For the case of a finite length cylinder with rigid ends the pressure is given by

$$P(x,r,\theta,t) = \sum_{m=0}^{\infty} Cos\left(\frac{m\ \pi\ x}{\mathrm{L}}\right) \left[\sum_{n=0}^{\infty} p^c_{nm}\ J_m(\lambda r)\ Cos\,(m\theta) + \sum_{n=1}^{\infty} p^s_{nm}\ J_m(\lambda r)\ Sin\,(m\theta) \right] e^{i\omega t} \tag{7}$$

were λ is given by $\lambda = \sqrt{\frac{\omega^2}{Co^2(1+i\ \eta_a)} - \left(\frac{m\pi}{L}\right)^2}$. The coefficients in the expression for the pressure, p^c_{nm} and p^s_{nm} are determined from the fluid boundary condition

$$\rho_a \frac{\partial \dot{W}}{\partial\ t} = \left.\frac{\partial P}{\partial\ r}\right|_{r=R} \tag{8}$$

where ρ_a is the density of air and the dot indicates velocity. Since the displacement, W, is a sine series in x and the pressure is a cosine series the boundary condition is enforced using a cosine series expansion of $W(x,r,\theta,t)$. Ultimately the cross spectral density of the coefficients of the acoustic pressure can be expressed as a complex transformation of the coefficients of the out-of-plane shell response. This is

$$S^{nm}_{pp} = Y^{ln}_{nm}\ S^{ln}_{aa} Z^{ln}_{nm} \tag{9}$$

were Y is the transpose of Z which is in general not square. The index n is the number of terms in the circumferential sine and cosine series in equations (4c) and (7) for the displacement and pressure respectively. The indices l and m are the number of terms in the longitudinal series expansions for the displacement and pressure respectively. These are generally not equal. The auto-spectra of the interior pressure can then be integrated over the volume of the cylinder and in frequency to form the objective function.

Optimization Problem

The objective of the optimization is to minimize the space averaged mean square interior sound pressure level in the cylinder normalized with respect to the baseline or uniform cylinder. The sole necessary constraint is that the core thickness be greater than or equal to zero everywhere. The objective is the noise reduction in decibels and is

$$Obj(d_i) \; = \; 10 \; Log_{10} \left(\int_0^R \int_0^L \int_0^{2\pi} \int_{fmin}^{fmax} \; \frac{S_{pp}(\; r, \; \theta, \; x, \; \omega \;)}{S_o} \; R \; d\theta \; dx \; dr \; d\omega \right) \tag{10}$$

where $S_{pp}(r, \theta, x, \omega)$ is the spectral density of the interior acoustic response and the normalization constant, S_o is chosen such that when $d_i = 0$ the objective is zero.

This objective function has historically been used for this type of study. This form offers the advantage of directly yielding the desired measure, noise reduction, but interjects several questionable points. Quite often the integrations are carried out numerically or by sampling and this leads to the inevitable convergence studies. This is a necessity in that in purely numerical solutions the time required and thus the actual feasibility of doing the optimization problems is directly proportional to the number of response locations. The presence of the log function in this formulation has two principal effects. The first is that the objective is zero when the design variables are zero. The second is that it tends to smooth the design space. This eases the gradients of the objective and broadens the minima. Both of these can add iterations to the minimization routines.

The physical interpretation of the only necessary constraint is that the core thickness, $H(\theta, d_i)$, be greater than or equal to zero. Since this is a continuous function of θ this inequality provides some difficulty in that there are several mathematical means of enforcing this. One of the most straightforward is to require the sum of the absolute value of the design variables to be less than unity. This is

$$\sum_{i=1}^{nvar} \mid d_i \mid \leq \;\; 1 \tag{11}$$

where nvar is the number of design variables and d_i are the design variables. This form of the constraint is, however, nonlinear and has discontinuity of slopes. A more verbose form of the necessary constraint but one that yields linear constraint equations is to construct the 2^{nvar} set of equations of all possible combinations of the variables and require them to be less than or equal to one. This simply expands the absolute value signs in equation (11) with all possible outcomes. A constraint screening method can then be employed in the optimization algorithm to omit inactive constraints.

Results

The results presented are for a cylinder of length twenty feet with a mean diameter of eight feet. The cylinder wall is constructed of aluminum honeycomb core with aluminum face sheets. The core has a mean thickness of one inch and a density of 0.001 lbs per inch cubed. The face sheets are each 0.02 inches thick. The interior space is assumed to be a standard atmosphere with the speed of sound of 1135 feet per second. Both the structural and acoustic regimes are assumed viscously damped to 5 percent of critical damping. The convection velocity of boundary layer noise is taken as sixty five percent of the free stream velocity which is Mach 0.7 . The remaining parameters of Corcos' boundary layer cross spectral density model are the same as in reference 4. The auto-spectrum of the turbulent boundary layer pressure is assumed constant over the frequency bands in these studies and is thus factored out of the objective function.

The allowable core thickness variation for these investigations was truncated to

$$H_{core}(d_i) = H_o \, (1 + d_3 Cos(3\theta) + d_4 Cos(4\theta) + d_5 Cos(5\theta) + d_6 Cos(6\theta)) \tag{12}$$

where the design space is four dimensional and continuous in $\varepsilon = \{d_3 \; d_4 \; d_5 \; d_6\}$ and bounded by $|d_3| + |d_4| + |d_5| + |d_6| \leq 1$. The $Cos(\theta)$ and $Cos(2\theta)$ terms were omitted from the thickness variation as preliminary results showed them to be of little value and the constant term was also omitted as this would change the cylinders weight. The optimization routine used was that provided for constrained minimization with the Matlab optimization tool box. For further details on this the reader is referred to reference 9.

The first step in presenting and discussing the results is to take a brief look at the baseline structure. Figures 2 and 3 do this. A graphical representation of the natural frequencies and mode numbers is shown in figure 2. This figure is symmetric indicating the presence of multiple resonances associated with the orthogonal sine and cosine solutions of the displacements in the circumferential direction. The choice of design variable in this investigation coupled the terms in the cosine expansion of the solutions and coupled terms in the sine expansion of the solution but do not couple the sine and cosine expansions themselves. This preserved the orthogonality of the P^c and P^s modal pressure responses and will be seen to limit the potential gains. The space averaged normalized acoustic response is shown in figure 3 for frequencies up to 1.4 kHz. From these two figures two frequency ranges were chosen in which to try and reduce the average noise levels. The first range from 125 Hertz to 175 Hertz is discussed in numerical experiment 1 while the second range from 240 Hertz to 290 Hertz is discussed in numerical experiment 2.

Numerical Experiment 1

The first numerical experiment was carried out over a frequency range from 125 Hertz to 175 Hertz. For the baseline structure the acoustic response in this range was dominated by a single large peak. The peak encompasses six resonant responses, two each at 152 , 154 and 155 Hertz. These have mode numbers (2,2), (1,5), and (3,4), respectively, where the first number in the bracket is the longitudinal order, m, and the second is the circumferential, n. The first optimization run was started with initial guess, $d_i = \{0.2\ 0.2\ 0.4\ 0.1\}$, were $i = 3, 4, 5,$ and 6. This is a feasible point away from the boundary of the design space. The optimizer converged to a point on the boundary of the design space. This point was $d_i = \{0.0\ 1.0\ 0.0\ 0.0\}$. The overall noise reduction achieved was 5.9 dB. The before and after spectra of the average interior noise level is plotted in figure 4 over the frequency range of the objective. It is easily seen that the dominant peak has been broken into three peaks with magnitudes over ten dB lower than the original. As a first step in examining the characteristics of the new design a graph of the natural frequencies of this cylinder is shown in figure 5. By comparing this with the uniform cylinder several observations can be made but first a brief discussion regarding required change in nomenclature. In the uniform cylinder a mode with a circumferential variation of four is comprised solely of a sine or cosine four theta term this is in general not true for a nonuniform cylinder. Thus the term fourth circumferential refers to a shape that is dominated by the four theta sine or cosine term. A mode whose dominant term is a cosine will possibly be comprised of any number of cosine terms but will not contain any sine terms. The same is true for a mode whose predominant shape is a sine term. This is due to the choice of the terms used in the expansion of the thickness. Thickness variations of solely sine or cosines do not couple displacement shapes of differing type. ie; sine or cosine theta.

The first observation regarding the changes in the natural frequencies of the optimized shell, figure 5., is the general stiffening of the cylinder. Most modes have higher resonant frequencies. It is further noted that the ring frequency has not changed. This is reasonable since the mean thickness of the shell is also unchanged. It is also observed that even and odd numbered circumferential modes behave differently. Odd numbered circumferential sine and cosine modes have the same resonant frequencies while even numbered circumferential sine and cosine modes do not. That is, figure 5 is symmetric about zero for odd n and unsymmetric for even n. The changes that are most significant to the noise reduction obtained is the changes in the second and fourth modes. Both sine and cosine terms in these modes are significantly lower in frequency. The fourth circumferential sine mode frequency is, however, much lower than its corresponding cosine mode. This selective shifting and separation of the resonances is the principal mechanism by which the noise level in this frequency band was reduced. A plot of a subset of the design space for the objective in this experiments was also made. The space is of $Obj(0, 0, d_5, d_6)$ with both d_5 and d_6 bounded. This space is shown in figure 6. There is little, however, that can be said regarding the overall space since the dominant design variable was d_4 but it is notable that the space is continuous and smooth and, as noted by other investigators, has local minima.

Numerical Experiment 2

As stated previously the frequency range of interest for this experiment was 240 Hertz to 290 Hertz. This range is just above the ring frequency of the uniform cylinder and is dominated by two spectral peaks. As before each peak is comprised of several resonances. Without going into great detail it is easily seen from figure 2 that there are many resonances in this range. The optimization routine was started with an initial guess of $d_i = \{0.1\ -0.2\ 0.2\ -0.1\}$ and converged to a final state of $d_i = \{0.0362\ 0.0089\ 0.0012\ -0.5514\}$ with a noise reduction of .59 dB. A first observation is that this is a nearly insignificant change in the interior environment however it is worthy of analysis to better understand the algorithms and physics of the problem. The before and after spectra of the objective show several interesting points. These spectra are shown in figure 7 and it is immediately seen that the first peak in the baseline spectrum has been completely removed by the optimization from the final spectrum. The second spectral peak, however, has increased in height. Though the overall noise level has decreased the optimized cylinder noise spectrum is potentially worse for crew fatigue and comfort. As these values for d_i looked rather arbitrary and were not near a boundary it was decided to restart the optimization from a nearby point closer to the constraint boundary. This point was $d_i = \{0.0362\ 0.0089\ 0.0012\ -0.8\}$. The optimization routine failed to advance from this point. The value of the objective indicated an overall noise reduction of .43 dB. This seems to indicate the presence of a large shallow and probably local minima in the design space. The plot of a subspace of the design space for this objective tends to confirm this assertion. This plot is of the subspace of the design space defined by $Obj(0, d_4, 0, d_6)$ subject to the bounds $|d_4| \leq 0.5$ and $|d_6| \leq 0.5$ and is shown in figure 8. The objective varies by no more than half a dB over this domain. This sub-domain also appears to have local minima.

Discussion

The structural and acoustic responses of a thick aluminum honeycomb core shell with aluminum face sheets and variable thickness core subjected to turbulent boundary layer noise were predicted by analytical methods. The core thickness variation was expressed as a four term cosine series in the circumferential direction. The series coefficients were used as design variable in two optimization studies. The objective in these studies was to minimize the volume and frequency averaged interior noise. The two investigations were carried out over two different frequency ranges using a commercially available optimization package. The basic finding of this work was that the interior noise levels could be reduced by this process sufficiently to warrant further study. The study also demonstrated the presence of multiple local minima in the design space and the detrimental nature of the typically used logarithmic objective function.

References

1. Cunefare, Kenneth A.; Crane, Scott P.; Engelstad, Stephen P.; and Powell, Eugene A.: "A tool for design minimization of aircraft interior noise."; AIAA/CEAS, Aeroacoustics Conference, 2nd, State College, PA, May 6-8, 1996; AIAA Paper 96-1702 (A96-30817)

2. Crane, Scott P.; Cunefare, Kenneth A.; Engelstad, Stephen P.; and Powell, Eugene A.: "A comparison of optimization formulations for design minimization of aircraft interior noise."; AIAA/ASME/ASCE /AHS/ASC, Structures, Structural Dynamics and Materials Conference, 37th, Salt Lake City, UT, Apr. 15-17, 1996; AIAA Paper 96-1480 (A96-26949)

3. Tang, Yvette Y.; Robinson, Jay H.; and Silcox, Richard J.: "Sound Transmission Through a Cylindrical Sandwich Shell With Honeycomb Core."; 34th AIAA Aerospace Sciences Meeting and Exhibit, January 15-18, 1996, Reno, NV. AIAA-96-0877.

4. Tang, Y. Y.; Silcox, R. J.; and Robinson, J. H.: " Modeling of Sound Transmission Through Shell Structures With Turbulent Boundary Layer Excitation."; Proceedings of The 1996 National Conference on Noise Control Engineering (NOISE-CON 96), September 29 - October 2, 1996, Bellevue, WA, Vol. I, pp. 171-176.

5. Fernholz, C. M.; and Robinson, J. H.: "An Investigation of the Influence of Composite Lamination Angle on the Interior Noise Levels of a Beech Starship."; Proceedings of The 1996 National Conference on Noise Control Engineering (NOISE-CON 96), September 29 - October 2, 1996, Bellevue, WA, Vol. II, pp. 809-814.

6. Fernholz, Christian M.; and Robinson, Jay H.: "The Influence of Lamination Angles on Interior Noise Levels of an Aircraft."; NASA TM 110250, August 1996.

7. Corcos, G. M.: "Resolution of Pressure in Turbulence"; J. Acoust. Soc. Am., Vol. 35(2), 1963, pp. 192-199.

8. Leissa, Arthur W.:"Vibration of Shells"; NASA SP 288, 1973.

9. Grace, Andrew:"Optimization Toolbox for Use with MATLAB"; The MathWorks, Inc., 1995.

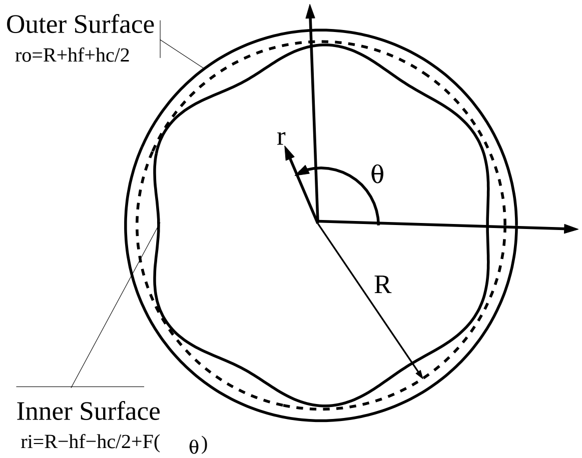

Figure 1. Geometry of variable thickness cylinder. Cylinder cross section view.

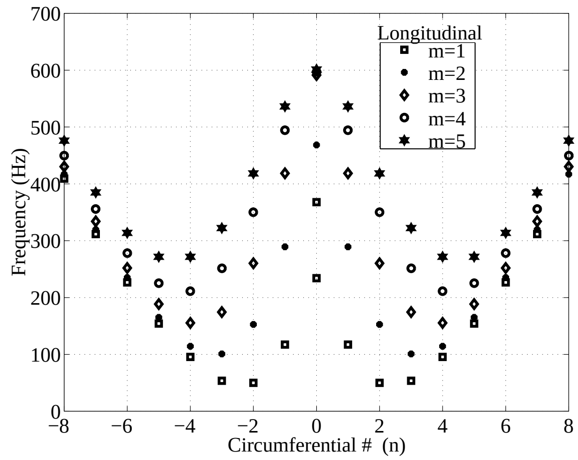

Figure 2. Graphical representation of the natural frequencies of uniform thickness cylinder. Positive values of n are the cosine θ modes and negative n are the sine θ modes.

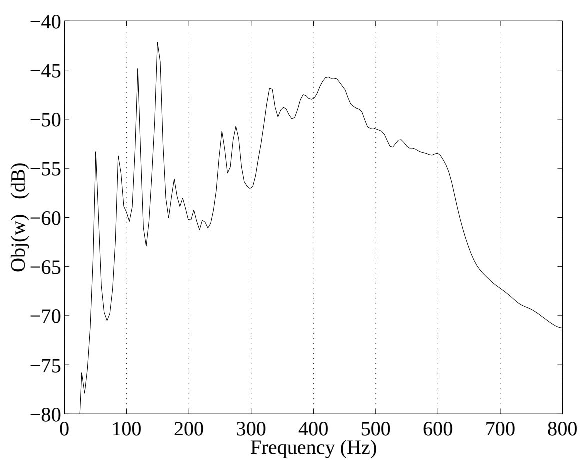

Figure 3. Space averaged interior noise spectrum for uniform thickness cylinder.

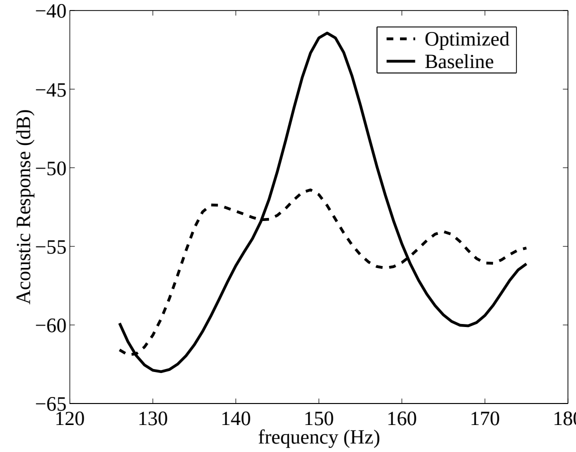

Figure 4. Before and After Space averaged interior noise spectrum for frequency range of objective in experiment 1.

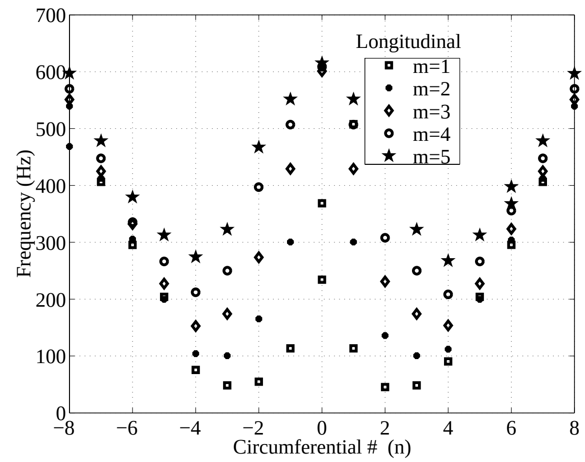

Figure 5. Graphical representation of the natural frequencies of optimized cylinder in experiment 1. Thickness variation is $H(\theta) = h_o\,[1 + Cos(4\ \theta)]$

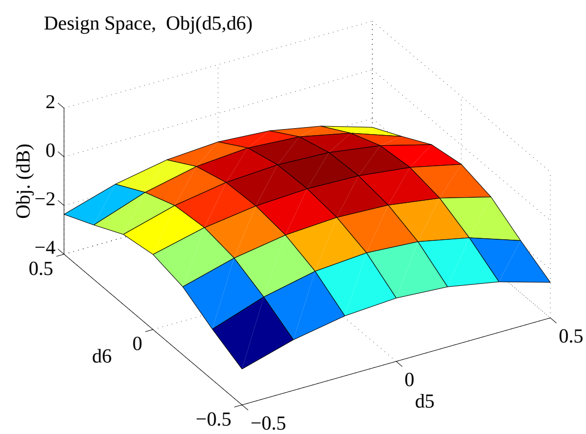

Figure 6. Subset of the design space for objective used in experiment 1.

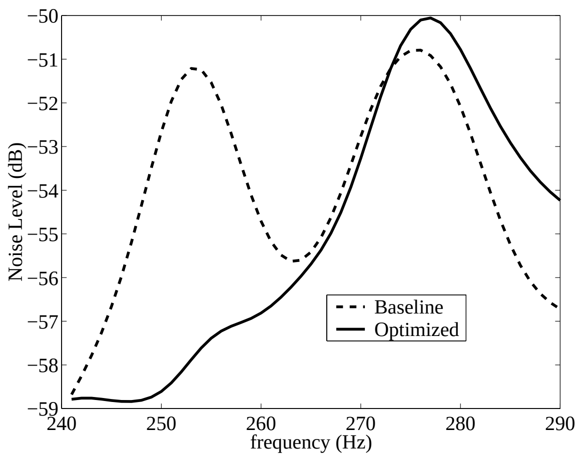

Figure 7. Before and After Space averaged interior noise spectrum for frequency range of objective in experiment 2.

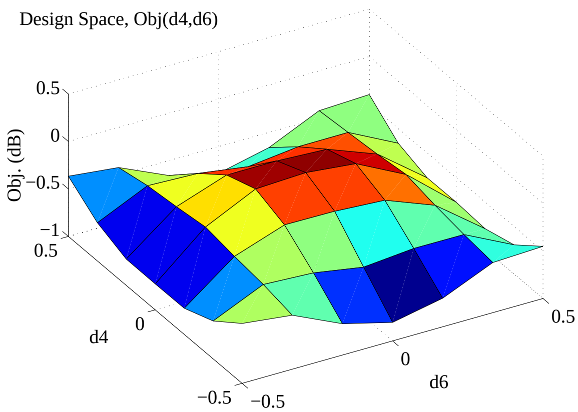

Figure 8. Subset of the design space for objective used in experiment 2.